Transformer Configuration in Three Dimensional Josephson Lattices at Zero Magnetic Field

Daniel Domínguez, Niels Grønbech-Jensen, and A. R. Bishop
Theoretical Division, MS B262, Los Alamos National Laboratory, Los Alamos, New Mexico 87545

Subodh R. Shenoy
International Center for Theoretical Physics, P.O. Box 586, Miramare, 34100 Trieste, Italy
(Received 27 February 1995)

Recent experiments on $Bi_2Sr_2CaCu_2O_{8-y}$ superconductors at zero magnetic field have been performed with a transformer configuration of contacts. We interpret the experimental data on the basis of large-scale Langevin dynamical simulations of a three dimensional (3D) Josephson lattice with a current bias through a single plane. We show that the experimentally observed effects can be attributed to linking thermal vortex loop excitations that cause voltages in neighboring superconducting planes to lock in a narrow temperature range near the 3D phase transition.

PACS numbers: 74.50.+r, 64.60.Cn, 74.60.Ge, 74.72.Hs

Giaever, in a pioneering "dc flux transformer" experiment showed that, with vortices linking two superconducting films, a current drive in the upper film induces locked voltages in both films [1]. A similar contact configuration has been used recently to study nonlocal transport properties of high-T_c superconductors [2–6]. In these experiments a current was fed into one *ab* face of a single crystal, and both the primary voltage drop (across the same face) and secondary drop (across the opposite face) were measured. Most of the experiments were performed in a magnetic field both in $Bi_2Sr_2CaCu_2O_x$ [2,6] and in $YBa_2Cu_3O_7$ [3,4], to probe vortex motion along the crystal **c** axis through the correlations between the primary and secondary voltages. The experimental results have been interpreted as due to a nonlocal conductivity [7] in the linear regime of the vortex liquid, and due to flux-line cutting phenomena [8] in the nonlinear regime below the irreversibility line. Recently, Wan *et al.* [5] have conducted transformer experiments at *zero* magnetic field in $Bi_2Sr_2CaCu_2O_{8-y}$, finding a peak in the secondary voltage around the critical temperature T_c. Here, we provide a theoretical interpretation of this latter experiment.

The high-T_c superconductors can be modeled by assuming that, below a mean field transition temperature T_c^{MF}, the relevant physics is given by the thermal fluctuations of the phase θ in the superconducting order parameter $\Psi = |\Psi| e^{i\theta}$. A lattice version of this approach leads to the anisotropic three dimensional (3D) *XY* model or Josephson lattice [9–13], the anisotropy arising from the layered nature of the high-T_c superconductors. This model has been extensively applied to the study of the thermodynamic phase transitions at both zero [9–11] and finite magnetic fields [12] in high-T_c superconductors.

The Hamiltonian of the 3D anisotropic *XY* model is

$$\mathcal{H} = -\sum_{\mathbf{r},\mu} J_\mu \cos \Delta_\mu \theta(\mathbf{r}), \tag{1}$$

where $\theta(\mathbf{r})$ is the phase at the 3D lattice site $\mathbf{r}$, $\Delta_\mu \theta(\mathbf{r}) = \theta(\mathbf{r} + \mu) - \theta(\mathbf{r})$, and $\mu = \hat{x}, \hat{y}, \hat{z}$. The anisotropy is $g_J = J_\perp / J_\parallel$, with $J_x = J_y = J_\parallel$ and $J_z = J_\perp$.

To study a current-driven sample, the flow of current has to be modeled taking into account local dissipation and that a time dependent phase induces a voltage $V = (\Phi_0/2\pi)(d\theta/dt)$, with $\Phi_0 = h/2e$, the quantum of flux. This is usually studied with current-conserving overdamped Langevin dynamics [13]. The current $I_\mu(\mathbf{r})$ flowing in each bond of the 3D cubic lattice is taken to be

$$I_\mu(\mathbf{r}) = \frac{\Phi_0}{2\pi \mathcal{R}_\mu} \frac{d\Delta_\mu \theta(\mathbf{r})}{dt} + I_{c,\mu} \sin \Delta_\mu \theta(\mathbf{r}) + \eta_\mu(\mathbf{r}, t), \tag{2}$$

with $I_{c,\mu} = 2\pi J_\mu / \Phi_0$, and $\mathcal{R}_\mu$ the resistance along the μ direction. We take $\mathcal{R}_x = \mathcal{R}_y = \mathcal{R}_\parallel$, $\mathcal{R}_z = \mathcal{R}_\perp$, and the anisotropy $g_R = \mathcal{R}_\parallel / \mathcal{R}_\perp$. We assume $g_J = g_R = g$, for simplicity, and we will study $g = 0.1$ here. The Langevin thermal noise term is assumed to have correlations $\langle \eta_\mu(\mathbf{r}, t) \eta_{\mu'}(\mathbf{r}', t') \rangle = (2k_B T / \mathcal{R}_\mu) \delta_{\mu,\mu'} \delta_{\mathbf{r},\mathbf{r}'} \delta(t - t')$. Together with the condition of current conservation,

$$\sum_\mu [I_\mu(\mathbf{r}) - I_\mu(\mathbf{r} - \mu)] = \Delta_\mu I_\mu(\mathbf{r}) = I_{\mathrm{ext}}(\mathbf{r}); \tag{3}$$

this determines the full set of dynamical equations. The boundary conditions, for the transformer configuration, are open along the x and z directions, periodic along the y direction, and current driven in the "top" plane $z = 1 : I_{\mathrm{ext}}(0, y, 1) = -I_{\mathrm{ext}}(L_x, y, 1) = I$ and $I_{\mathrm{ext}}(\mathbf{r}) = 0$ otherwise. From (2) and (3) we obtain

$$\frac{d\theta(\mathbf{r})}{dt} = \frac{2\pi}{\Phi_0} \sum_{\mathbf{r}'} G(\mathbf{r}, \mathbf{r}') \times \left[I_{\mathrm{ext}}(\mathbf{r}') + \frac{2\pi}{\Phi_0} \frac{\delta \mathcal{H}}{\delta \theta(\mathbf{r}')} - \Delta_\mu \eta_\mu(\mathbf{r}', t) \right]. \tag{4}$$

Here the 3D Green's function is the solution of $\Delta_\mu (1/\mathcal{R}_\mu) \Delta_\mu G(\mathbf{r}, \mathbf{r}') = \delta_{\mathbf{r},\mathbf{r}'}$ under the given boundary conditions. Thus the information of the anisotropy in the resistance network is contained both in $G(\mathbf{r}, \mathbf{r}')$ and in the correlations of $\eta_\mu(\mathbf{r}, t)$. We simulate Eq. (4) both with a Fourier accelerated algorithm [14] and with a

molecular dynamics algorithm [15], previously used in 2D networks. We integrate (4) with the Helfand-Greenside [16] algorithm with $\Delta t = 0.05\tau$ ($\tau = \Phi_0/2\pi\mathcal{R}_\parallel I_{c,\parallel}$) and the integration time $t = 10^4\tau$ after a transient of $2 \times 10^3\tau$.

We study first the equilibrium behavior. We obtain the 3D critical temperature T_c by calculating the helicity modulus $\Upsilon_{\rm eq}$ along the xy directions [10] (see Fig. 1). We obtain $T_c \approx 1.33$ for a $48 \times 48 \times 8$ lattice, with periodic boundary conditions in order to obtain better statistics. (Temperatures are normalized by $J_\parallel/k_B$.) Recently, Chattopadhyay and Shenoy [11] have shown that, for $g_J \lesssim 0.25$, below the 3D T_c there is a *crossover* temperature $T_{\rm KT}$ reminiscent of the Kosterlitz-Thouless phase transition in 2D [17]. We found this crossover temperature by studying the nonlinear I-V characteristics with homogeneous bias current, with the same procedure as in the experiment of [5]: $T_{\rm KT} \approx 1.0$. We do not see evidence of structure in the helicity modulus at $T_{\rm KT}$ [11]. Here, we have neglected the temperature dependence of J_μ, which is $J_\mu(T) \sim T_c^{\rm MF} - T$ for $T \sim T_c$. The effect of a T-dependent J_μ is to "squeeze" the temperature interval around T_c, making $T_{\rm KT}$ and T_c very close, as in the experiment [5]. By neglecting such T dependence we can conveniently separate the effect of both temperatures.

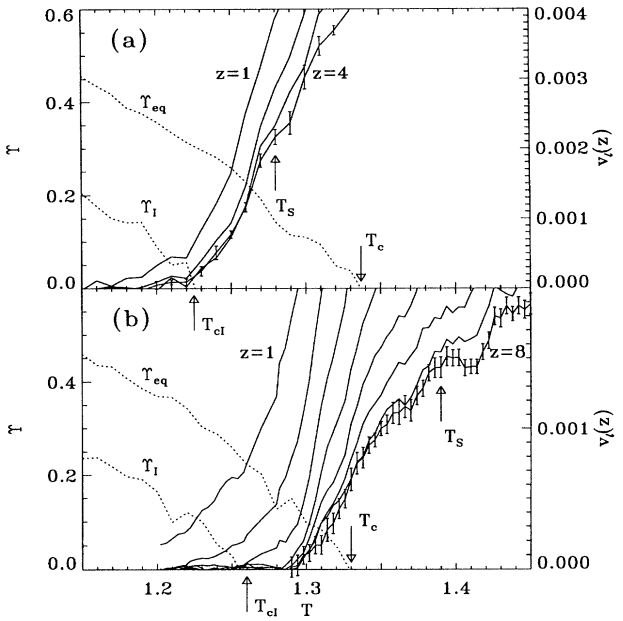

FIG. 1. Left scale, dotted lines helicity modulus without a current bias $\Upsilon_{\rm eq}$ and with a bias in the transformer configuration Υ_I calculated along the x direction. Right scale, full lines: voltages $v_\ell(z)$ as a function of temperature T (normalized by $J_\parallel/k_B$), for $\ell = 6$. The voltages decrease from the top plane $z = 1$ to the bottom plane $z = L_z$. (a) $48 \times 48 \times 4$ lattice. (b) $48 \times 48 \times 8$ lattice. Bias $I = 0.1I_{c,\parallel}$. Numerical results taken in steps of $\Delta T = 0.04$. Error bars are shown on the $z = L_z$ curves.

Under the transformer configuration, a bias current is applied in the top plane and voltage differences are measured in the top ($z = 1$) and bottom ($z = L_z$) planes. We calculate the average normalized voltages $v(x,z) = (\tau/L_y)\sum_y\langle\dot\theta(x,y,z,t)\rangle$, where $\langle\cdots\rangle$ indicates thermal (time) average. Because of the inhomogeneous bias, the voltages depend strongly on (x,z), and therefore the results depend on where the voltage differences are measured. We study $v_\ell(z) = v(L_x - \ell, z) - v(1 + \ell, z)$. In the high-temperature limit $T \gg T_c$ the behavior is purely resistive, and the local voltage differences $v_\mu(\mathbf{r}) = \Delta_\mu v(\mathbf{r})$ are simply given by $v_\mu(\mathbf{r}) = (2\pi\tau/\Phi_0)\Delta_\mu\sum_{\mathbf{r}'} G(\mathbf{r},\mathbf{r}')I_{\rm ext}(\mathbf{r}')$, which explicitly shows the role of $G(\mathbf{r},\mathbf{r}')$. In this case it is easy to see that most of the current flow between planes (along the z direction) occurs in a small region close to the edges. Therefore $v_\ell(z)$ depends strongly on ℓ for $\ell < L_x g_R/\pi$, and otherwise is approximately ℓ independent. The voltages decrease exponentially along the z direction as $v_\ell(z) \sim \exp(-z/z_{\rm eff})$ with $z_{\rm eff} = L_x g_R^{1/2}/\pi$.

In Fig. 1 we show the voltage differences $v_\ell(z)$ in all the planes, as a function of T for samples of size $L_x = L_y = 48$ and increasing length along z, for $L_z = 4$ and $L_z = 8$. The bias current is applied only along the top plane, and in this case is $I = 0.1I_{c,\parallel}$. We see that at a temperature $T_{cI}(I, L_z) < T_c$ dissipation begins in the bottom plane. This is close to the temperature where the helicity modulus Υ_I of the current driven lattice, calculated along the x direction [18], vanishes; see Fig. 1. Here $T_{cI}(0.1, 4) = 1.23$, $T_{cI}(0.1, 8) = 1.27$. We find that $T_{cI} \to T_c$ for $I \to 0$ or for $L_z \to \infty$, for the currents and sizes we studied. The top plane begins to dissipate at a much lower temperature, depending strongly on ℓ (decreasing for increasing ℓ, and approaching T_{cI}), meaning that it is due to the onset of dissipation in the junctions close to the edge of the sample. Figure 1 shows that while only the $z = 1$ plane is driven voltages are induced in all the planes. Within some temperature interval $T_{cI} < T < T_S(z)$, there is a tendency for voltages to crowd together or lock within the error bars (shown for the $z = L_z$ curve). The largest unlocking temperature where $v(L_z) \neq v(L_z - 1)$ within the statistical error $T_S = T_S(L_z)$ is shown. *This voltage-locking tendency away from the current-driven plane is the essential aspect of the transformer effect.* When we increase the number of planes from $L_z = 4$ to $L_z = 8$ [see Fig. 1(b)], we see a tendency that the voltage $v_\ell(L_z)$ will drop after $T > T_S$. (Also, by increasing L_z the system becomes more three dimensional; see, for example, Schmidt and Schneider [10].) We also calculated the average normal current $i_N^{z,z+1}$ and Josephson current $i_J^{z,z+1}$ flowing between planes $z, z+1$. An analysis of $\gamma(z,T) = i_N^{z,z+1}/i_J^{z,z+1}$ for $z > z_{\rm eff}$ shows that $\gamma \approx 0$ below T_{cI}, $0 < \gamma < 1$ for $T_{cI} < T < T_S$, and γ increases sharply above T_S. Thus, the dissipation in the lower planes for $T_{cI} < T < T_S$

is mainly due to vortex loop motion and not to normal current leakage.

Our interpretation of these results is as follows. The thermodynamic phase transition in the 3D XY model is driven by multiplane vortex loop excitations of size $\xi_- \sim (T_c - T)^{-\nu}$ that "blow out" in a narrow interval around T_c [9]. For $T_c < T < T_S$, there are vortex loops or lines that extend across a finite sample, with "stiff" regions of size $\xi_+ \sim (T - T_c)^{-\nu}$, capable of inducing correlated voltages in the lower planes if the top plane is current driven. These induced voltages will rise as vortex fugacities rise with T, and may fall as stiffness decreases. (This simple scenario is masked for planes closer to $z = 1$ by single plane excitations [11] on scales $r_0 \sim g_J^{-1/2}$, and interplane current leakage effects.) Above T_S, where normal current flow dominates [$\xi_+(T) \lesssim z_{\rm eff}$], $v_\ell(L_z)$ drops from $v_\ell(L_z) \approx v_\ell(L_z - 1)$ towards its normal state value $v_\ell(L_z) \approx v_\ell(L_z - 1)\exp(-1/z_{\rm eff})$. This last effect is stronger for increasing L_z [compare Figs. 1(a) and 1(b)] or smaller g_R. Therefore, we expect that the weak peak seen in Fig. 1(b) will grow with increasing sample thickness or with stronger anisotropy in the *resistivity*. This may explain the experiment of Wan *et al.* [5]. There, they observed a peak in the secondary voltage $v_\ell(L_z)$ for temperatures between 85.5 and 87.5 K and their 3D critical temperature was $T_c = 86.4$ K. In their case the Kosterlitz-Thouless crossover was very close to the peak but clearly below it, at $T_{\rm KT} = 84.3$ K. As is clear from our results $T_{\rm KT}$ plays little role in the peak in $v_\ell(L_z)$.

To verify this scenario, we have calculated the distribution of the vortex segments defined as $N_\mu(\mathbf{R}) = -\Delta_\nu^\mu \,\mathrm{nint}[\Delta_\nu \theta(\mathbf{r})/2\pi]$, with $(\mathbf{R}, \mu)$ labeling the dual lattice site $\mathbf{R}$ oriented along the μ direction. The lattice curl operator is, for example, $\Delta_\nu^z \times \Psi_\nu(\mathbf{R}) = \Psi_x(\mathbf{r}) - \Psi_x(\mathbf{r} + \hat{y}) + \Psi_y(\mathbf{r} + \hat{x}) - \Psi_y(\mathbf{r})$, and nint$(x)$ denotes the nearest integer part of x. The z component $N_z(\mathbf{R})$ can be either positive or negative ($N_z^{(\pm)} = \pm 1$). Vortex loop closure implies $\sum N_z^{(+)}(\mathbf{R}) + N_z^{(-)}(\mathbf{R}) = 0$, so we evaluate the separate correlations $C^{(\pm)}(\mathbf{R}_\parallel; \mathbf{r}_\parallel, z) = \langle N_z^{(\pm)}(\mathbf{R}_\parallel, L_z) N_z^{(\pm)}(\mathbf{R}_\parallel + \mathbf{r}_\parallel, L_z - z)\rangle$, with $\mathbf{r}_\parallel = (x, y)$. $C^{(\pm)}$ depends on $\mathbf{R}_\parallel$ because of the lack of translational invariance. We average over $0 < R_y < L_y$ and $\ell < R_x < L_x - \ell$. The $N_z^{(+)}$ segments connected on the same loop are not necessarily right on top of each other in the different z planes. Therefore, we sum over $\mathbf{r}_\parallel$ within a cylinder $|\mathbf{r}_\parallel| < \rho$. Substracting the independent thermal averages $A^{(\pm)}(\mathbf{R}_\parallel; \mathbf{r}_\parallel, z) = \langle N_z^{(\pm)}(\mathbf{R}_\parallel, L_z)\rangle \langle N_z^{(\pm)}(\mathbf{R}_\parallel + \mathbf{r}_\parallel, L_z - z)\rangle$,

$$c_{\ell,\rho}(z) = \frac{1}{(L_x - 2\ell)L_y} \sum_{x,y=0}^{\rho} \sum_{R_x=\ell}^{L_x-\ell} \sum_{R_y=1}^{L_y} C^{(+)}(\mathbf{R}_\parallel; \mathbf{r}_\parallel, z) - A^{(+)}(\mathbf{R}_\parallel; \mathbf{r}_\parallel, z) + C^{(-)}(\mathbf{R}_\parallel; \mathbf{r}_\parallel, z) - A^{(-)}(\mathbf{R}_\parallel; \mathbf{r}_\parallel, z)\,.$$

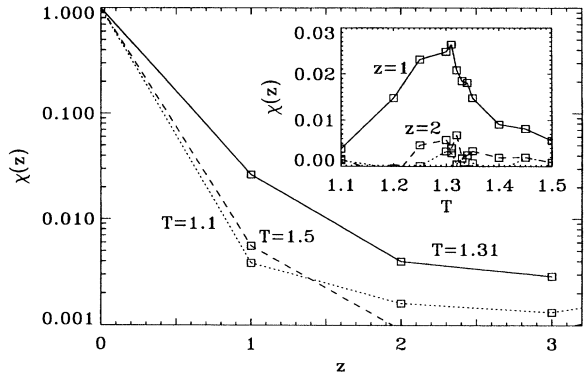

FIG. 2. Correlation function $\chi(z, T)$, defined in the text, as a function of z: $T = 1.1$ (dotted line), $T = 1.31$ (full line), and $T = 1.5$ (dashed line). Inset: $\chi(z, T)$ as a function of T, for $z = 1$ (full line), $z = 2$ (dashed line), and $z = 3$ (dotted line). Lattice size is $48 \times 48 \times 8$.

The dimensionless ratio $\chi_{\ell,\rho}(z) = c_{\ell,\rho}(z)/c_{\ell,\rho}(0)$ is thus a measure of the "stiffness" of the vortex segments, unity for rigid rods. In Fig. 2 we plot $\chi_{\ell,\rho}(z, T)$ for $\ell = 8$, $\rho = 3$, and for three different temperatures: below, at, and above the transformer region. In the inset of Fig. 2 we show $\chi(z, T)$ as a function of T for $z = 1, 2$, and 3. It shows a peak at T_c in a temperature interval coinciding with the region where we found a transformer coupling effect in Fig. 1, thus confirming our interpretation. This makes evident the strong correlations between vortex segments in the transformer region. In Fig. 3 we show the distribution of $N_\mu(\mathbf{R})$ at temperatures below and at the transformer region. For $T < T_{cl}$ there are only small vortex loops, and

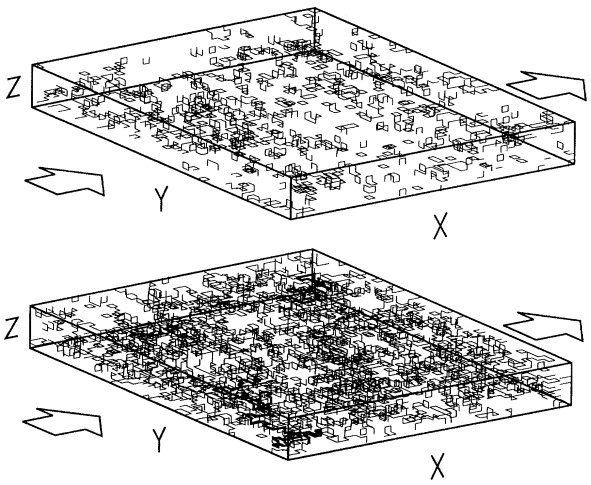

FIG. 3. Distribution of vortex segments in the Josephson lattice of size $48 \times 48 \times 8$, with a bias $I = 0.1 I_{c,\parallel}$ along the x direction in the plane $z = 1$. Top: $T = 1.15$. Bottom: $T = 1.31$. Some vortex loops or lines that extend from the bottom to the top plane are highlighted.

therefore no coupling between planes. For $T_{cl} < T \sim T_c$ there is a proliferation of loops of different sizes and shapes. In the figure we highlight some vortex loops or lines extending from the bottom to the top plane.

In the experiments on the flux transformer effect in an external magnetic field, the results have been interpreted as evidence of a nonlocal resistivity in the system [3,7]. In our model this means that the average voltage drop in a given lattice link will be $V_\mu(\mathbf{r}) = \sum_{\mathbf{r}',\mu'} \mathcal{R}_{\mu,\mu'}(\mathbf{r},\mathbf{r}') I_{\mu'}(\mathbf{r}')$. It is easy to show that in the Josephson lattice this is given in general by

$$\mathcal{R}_{\mu,\mu'}(\mathbf{r},\mathbf{r}') = \mathcal{R}_\mu \left[\delta_{\mu,\mu'}\delta_{\mathbf{r},\mathbf{r}'} - I_{c,\mu} \frac{\partial \langle \sin \Delta_\mu \theta(\mathbf{r}) \rangle}{\partial I_{\mu'}(\mathbf{r}')} \right]. \tag{5}$$

Clearly the nonlocal part becomes relevant as soon as there are correlations between the $\theta(\mathbf{r})$, i.e., vortex loops occur. One can estimate that the Fourier transform of the resistance for small wave vector q will be of the form $\mathcal{R}(q) \sim \mathcal{R}_0 + \mathcal{R}_2(q\xi)^2$, thus the nonlocal part is relevant for large ξ as we discussed previously.

In our calculations we have neglected the magnetic interactions between planes. They are not relevant to the essential nature of the transition at T_c. However, in the experiment of Wan *et al.* [5], they are present since the magnetic penetration depth is smaller than the sample size $\lambda_{ab} < L_x$. This will result in a stronger effective interaction between vortex segments in different planes, making the vortex loops "stiffer," and thus the coupling effect will be enhanced when compared to our results with the 3D *XY* model. The magnetic interactions and screening effects are qualitatively relevant, however, for the interpretation of experiments at weak magnetic fields, $H \lesssim H_{c1}$, like the ones recently conducted in Ref. [6].

The transformer effect discussed here should also be present in isotropic or weakly anisotropic systems, like $YBa_2Cu_3O_7$. The difference is that there will be a less prominent drop in $v_\ell(L_z)$ above T_c, probably similar to the one shown in Fig. 1(b). The coupling between planes can be studied by testing the nonlocality of the resistance in a narrow region around T_c, following the same procedure as [3] for $YBa_2Cu_3O_7$ in a magnetic field.

In conclusion, we have shown that at zero magnetic field there is a coupling between the superconducting planes around the 3D *XY* phase transition. This constitutes the essence of the effects observed in the zero field transformer experiments [5]. The coupling between planes is due to correlated segments of thermal vortex excitations. The role of the anisotropy in the resistivity is to cause a drop in the secondary voltage at temperatures above T_c. It also produces a very inhomogeneous distribution of currents in the sample, and thus the results depend on the location of the voltage contacts, especially close to the sample edges. The crossover temperature T_{KT} [11] does not seem to be relevant to our results. To fully understand all these phenomena, further detailed studies of the current driven 3D *XY* model and extensions to include a magnetic field are in progress.

[1] I. Giaever, Phys. Rev. Lett. **15**, 825 (1965).

[2] H. Safar *et al.*, Phys. Rev. B **46**, 14 238 (1992); R. Busch *et al.*, Phys. Rev. Lett. **69**, 522 (1992).

[3] H. Safar *et al.*, Phys. Rev. Lett. **72**, 1272 (1994).

[4] D. López *et al.*, Physica (Amsterdam) **194-196B**, 1977 (1994); D. López, G. Nieva, and F. de la Cruz, Phys. Rev. B **50**, 7219 (1994).

[5] Y. M. Wan *et al.*, Phys. Rev. Lett. **71**, 157 (1993).

[6] Y. M. Wan, S. E. Hebboul, and J. C. Garland, Phys. Rev. Lett. **72**, 3867 (1994).

[7] D. A. Huse and S. N. Majumdar, Phys. Rev. Lett. **71**, 2473 (1993); T. Blum and M. A. Moore, (to be published); C. Y. Mou *et al.* (to be published).

[8] D. López *et al.*, Phys. Rev. B **50**, 9684 (1994); K. K. Uprety and D. Dominguez, Phys. Rev. B **51**, 5955 (1995); D. O'Kane and H. J. Jensen, Physica (Amsterdam) **235-240C**, 2619 (1994); W. Yu and D. Stroud (to be published).

[9] G. Williams, Phys. Rev. Lett. **59**, 1926 (1987); S. R. Shenoy, Phys. Rev. B **40**, 5056 (1989).

[10] W. Janke and T. Matsui, Phys. Rev. B **42**, 10 673 (1990); P. Minnhagen and P. Olsson, Phys. Rev. Lett. **67**, 1039 (1991); A. Schmidt and T. Schneider, Z. Phys. B **87**, 265 (1992).

[11] B. Chattopadhyay and S. R. Shenoy, Phys. Rev. Lett. **72**, 400 (1994); S. R. Shenoy and B. Chattopadhyay, Phys. Rev. B **51**, 9129 (1995).

[12] Y. H. Li and S. Teitel, Phys. Rev. Lett. **66**, 3301 (1991); Phys. Rev. B **49**, 4136 (1994).

[13] See, for example, K. H. Lee, D. Stroud, and S. M. Girvin, Phys. Rev. B **48**, 1233 (1993); R. Sugano, T. Onogi, and Y. Murayama, Phys. Rev. B **48**, 13 784 (1993).

[14] D. Dominguez *et al.*, Phys. Rev. Lett. **67**, 2367 (1991).

[15] F. Falo, A. R. Bishop, and P. S. Lomdahl, Phys. Rev. B **41**, 10 983 (1990).

[16] H. S. Greenside and E. Helfand, Bell. Syst. Tech. J. **60**, 1927 (1981).

[17] $g_J < 0.25$ corresponds to the strong anisotropy regime of the 3D *XY* model, see [11]. We choose $g_J = 0.1$ as a representative of strongly anisotropic superconductors.

[18] Υ_l was calculated along the direction parallel to the current, with the same definition of the helicity modulus used for the zero-current case. For Υ_y, along the direction perpendicular to the current, we obtain $\Upsilon_y \approx \Upsilon_{eq}$, but vanishing slightly below T_c.